# Origin of Non-Uniformity of the Source Plasmas in JT-60 Negative Ion Source*)

Masafumi YOSHIDA, Masaya HANADA, Atsushi KOJIMA, Takashi INOUE, Mieko KASHIWAGI, Larry R GRISHAM[1)], Noboru AKINO, Yasuei ENDO, Masao KOMATA, Kazuhiko MOGAKI, Shuji NEMOTO, Masahiro OHZEKI, Norikazu SEKI, Shunichi SASAKI, Tatsuo SHIMIZU and Yuto TERUNUMA

*Japan Atomic Energy Agency, 801-1 Mukoyama, Naka 311-0193, Japan*
[1)]*Princeton Plasma Physics Laboratory, Princeton, USA*

(Received 6 December 2012 / Accepted 14 August 2013)

In order to investigate the origin of the non-uniformity of the source plasmas in the JT-60 negative ion source, the distribution of $H^+$ ions and $H^0$ atoms, which were converted to $H^-$ ions on the cesium covered surface, were measured by Langmuir probes and emission spectroscopy. Both of $H^+$ ions and $H^0$ atoms at the top and bottom of the ion source were about twice higher and lower than those in the center region, respectively. In particular, they were highly localized near the side wall of the top of the ion source. The analyses of the primary electron trajectories showed that this non-uniformity was due to the B x grad B drift of primary electrons emitted from filaments. These results suggest that the non-uniformity of the negative ions results in a locally poor beam optics and significant direct interception of the $H^-$ ions on the acceleration grid. This is the reason why the negative ion beams are non-uniform in the JT-60 negative ion source.



Keywords: negative ion source, neutral beam injection, arc discharge, Langmuir probe and emission spectroscopy

DOI: 10.1585/pfr.8.2405146

## 1. Introduction

The negative ion based neutral beam (N-NB) injection is one of the promising candidates for plasma heating and plasma current drive with high efficiency in fusion devices. In JT-60SA, the beam current per ion source and pulse duration time are required to be 22 A at 500 keV and 100 s, respectively [1, 2]. The high current beam is produced in the largest negative ion source in the world that has a semi-cylindrical arc chamber of 640 mm in diameter and 1220 mm in length, and acceleration grids with an area of 450 mm in width × 1100 mm in length [3]. In the arc chamber, $H^+/D^+$ ions and $H^0/D^0$ atoms are produced and converted to $H^-/D^-$ ions on the surface with cesium coverage. Therefore, it is required to produce $H^+/D^+$ ions and $H^0/D^0$ atoms uniformly in the large arc chamber. Otherwise, the beam optics is locally degraded, resulting in a significant grid power loading [4, 5].

In the previous operation of the JT-60 negative ion source, the non-uniformity of the accelerated $D^-$ ion beams had been observed. In particular, the beam intensity was extremely weak at the top and bottom of the ion source. The acceleration grid was also observed to be locally melted [4, 5]. These indicate a spatial non-uniformity of the negative ions in the arc chamber. However, the origin of the non-uniformity has not been clarified yet.

In order to clarify the origin of the non-uniformity of the negative ions in the large negative ion source, distributions of the $H^+$ ions and $H^0$ atoms giving the parent particles of the $H^-$ ions are carefully measured in the JT-60 negative ion source. The $H^+$ ions are measured by Langmuir probes, and the $H^0$ atoms are evaluated from the measurement of H$\alpha$ line emission. The trajectories of the primary electrons emitted from filaments are also calculated to understand the origin of the non-uniformity of the plasma in the arc chamber.

In this paper, the origin of the non-uniformity in the large negative ion source is reported.

## 2. Experiment and Experimental Apparatus

### 2.1 JT-60 negative ion source

Figure 1 shows schematic view of the arc chamber and the extractor of the JT-60 negative ion source and the experimental apparatus. The coordination of the arc chamber is taken as shown in this figure. In the JT-60 negative ion source, the arc chamber is fully surrounded by 26 rows of permanent magnets on the side wall and 10 rows of permanent magnets on top and bottom of wall. In addition, the so-called PG magnetic filter is created by flowing current into the plasma grid longitudinally in order to enhance the

*author's e-mail: yoshida.masafumi@jaea.go.jp*
*) This article is based on the presentation at the 22nd International Toki Conference (ITC22).

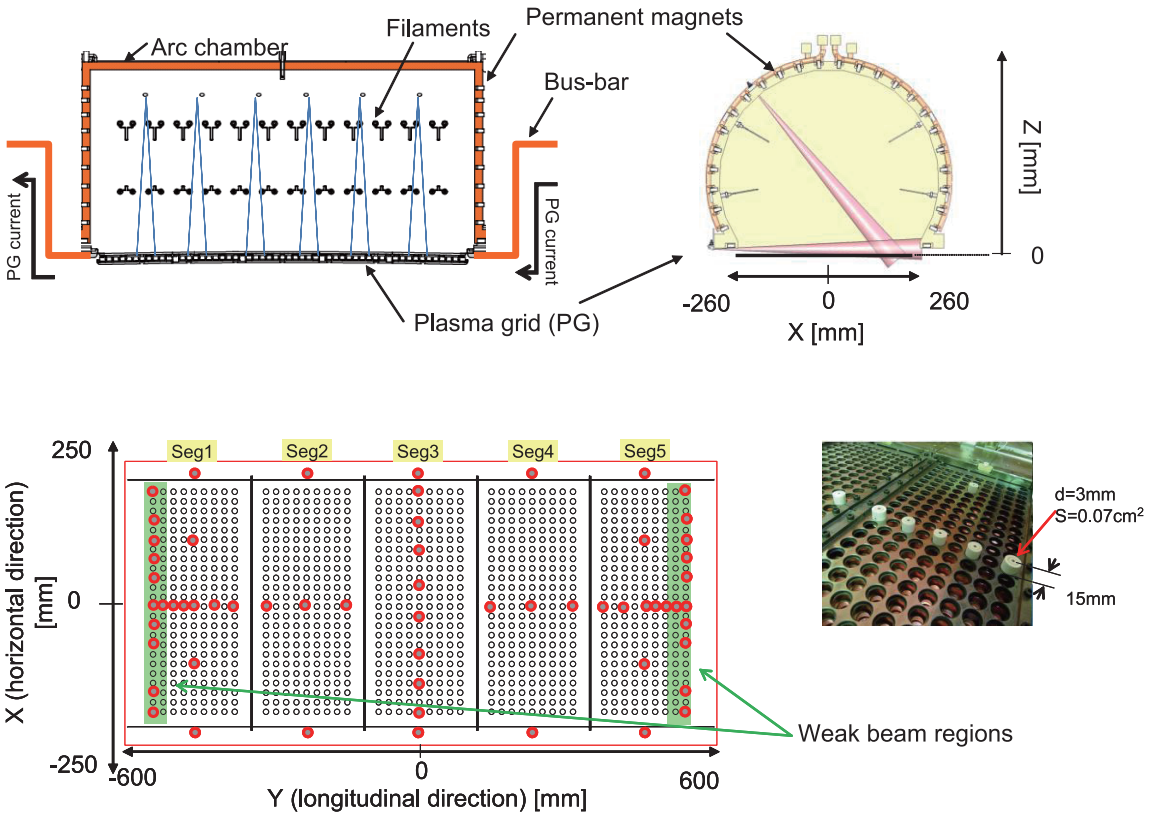


Fig. 1 Schematic view of longitudinal and horizontal cross-section of JT-60 negative ion source. The positions of the Langmuir probes and line of the sight in emission spectroscopy are shown in this figure.

negative ion production. Magnets are also installed in an extraction grid (EXG) to suppress the acceleration of the extracted electrons with the negative ions.

The negative ions are extracted from an ion extraction area of $-228\,\mathrm{mm} < X < 228\,\mathrm{mm}$, and $-580\,\mathrm{mm} < Y < 580\,\mathrm{mm}$, where there are 1080 apertures of 14 mm in diameter.

The filaments are located at 50 mm from the side wall. Figure 2 (a) shows positions of the filaments and vector diagram of the magnetic field of $XZ$-plane at $Y = 45$ mm with PG filter current of 5 kA. The filaments are set in the strong magnetic fields of 15 - 70 Gauss.

In this experiment, the arc chamber was operated at 0.3 Pa and at an arc power of 100 kW.

## 2.2 Diagnostics

The plasma parameters, such as ion saturation current ($J_{is}$), electron temperature and density were measured by 52 Langmuir probes, which are made of Mo with surface area of $0.07\,\mathrm{cm}^2$ ($\phi = 3$ mm). The probes were located at 15 mm apart from the PG surfaces in Fig. 1. The light intensity of plasma in the longitudinal direction was measured through 6 optical fibers by spectroscopy. The measured spectral is ranged in 400 - 700 nm.

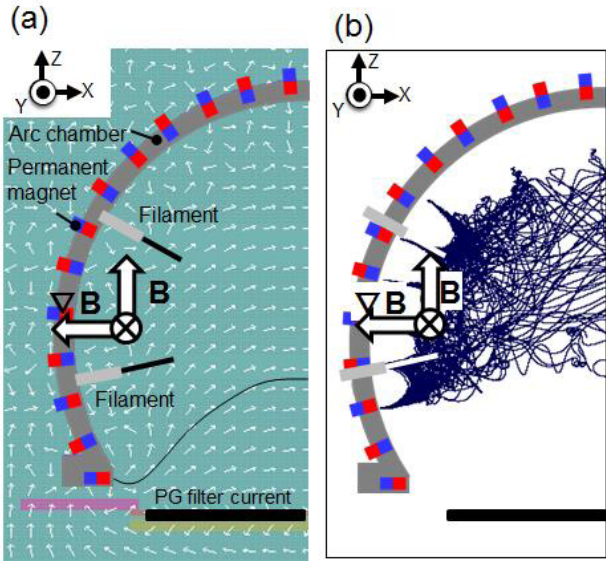


Fig. 2 (a) Vector diagram of the magnetic field of $XZ$-plane at $Y = 45$ mm with PG filter current of 5 kA and (b) typical trajectories of the electrons.

# 3. Calculated Population of the Primary Electrons in the Arc Chamber

Magnet fields around the filaments are mainly formed by combining the cusp magnet filter with the PG one as

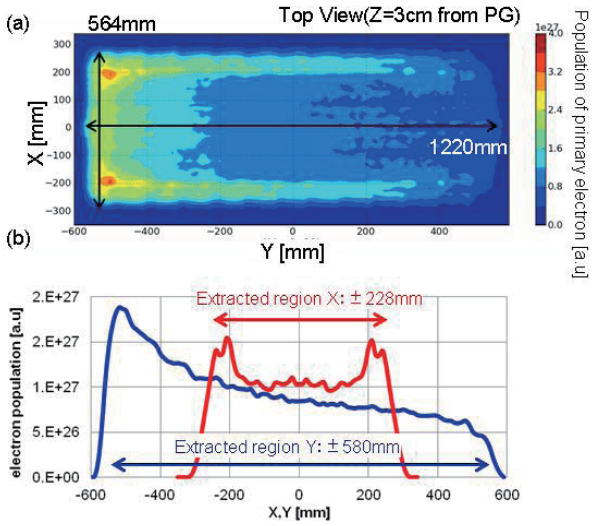


Fig. 3 (a) Calculated contour-map of the population of the primary electrons in the $XY$ plane by calculation, and (b) population of the primary electron in the longitudinal direction ($Y = -550$ mm) and in the horizontal direction ($X = 0$ mm).

shown in Fig. 2 (a). These magnetic fields are produced in the whole arc chamber. The filaments are located in relatively strong magnetic field, which leads to localization of the primary electrons emitted from the filaments. To clarify the influence on the magnetic field, the trajectories of the primary electrons was calculated by the Magnum for 3D finite-element magnetostatic calculation codes and Omni Trak codes [6]. The primary electrons are assumed to be emitted from the filaments with the arc voltage of −100 V [7].

Figure 2 (b) shows typical trajectories of the electrons emitted from the filaments. It is clearly shown that most of the primary electrons emitted from the filaments are strongly trapped by the magnetic fields around the filaments and are drifted toward the top of the arc chamber by B x grad B.

The drift of the primary electrons are shown in Fig. 3 (a) of the contour-map of the population of the primary electrons in $XY$ plane. The contour-map is determined by integration of the primary electron trajectory along the $Z$ direction. Figure 3 (b) shows the populations in the longitudinal direction at $X = 0$ mm and in the horizontal direction at $Y = -550$ mm. These populations are determined by integration of the primary electron trajectory along the $Z$ direction. It is clearly shown that the primary electrons emitted from filaments are drifted toward the top through the side wall of the arc chamber by B x grad B and are locally distributed at the top of the arc chamber in the longitudinal direction. They are significantly localized at the corner of the top in the horizontal direction. The similar tendency of the primary electrons is observed in the JAEA 10 A negative ion source [8] where the plasma is localized in the top of the arc chamber. This suggests that the source plasma could be non-uniform in the JT-60 negative ion source.

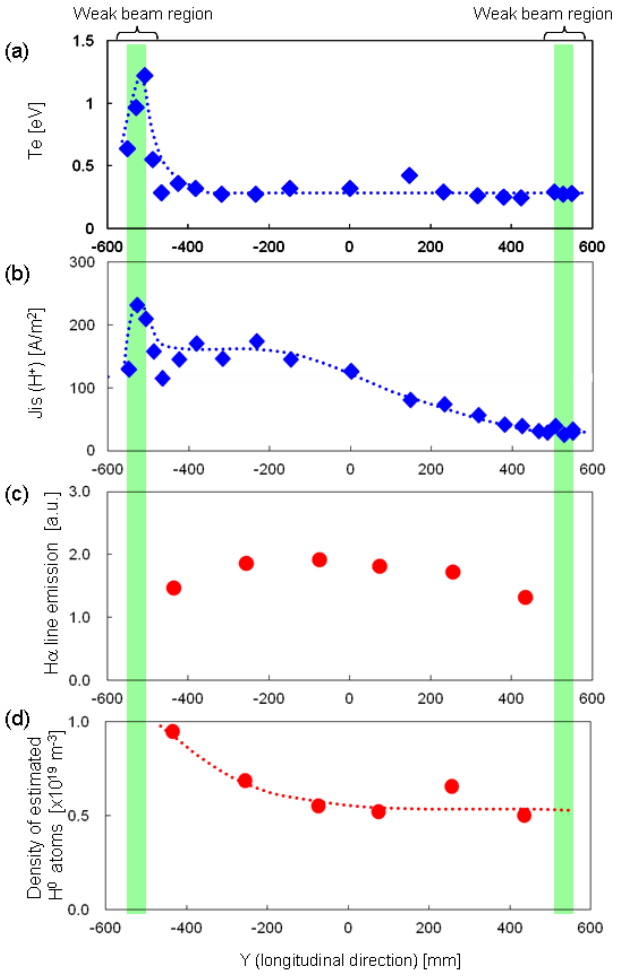


Fig. 4 Typically longitudinal distributions of (a) electron temperature ($T_e$), and (b) the ion saturation current ($J_{is}$ ($H^+$)) measured at $X = 0$ mm and $Z = 15$ mm by the Langmuir probes, and (c) intensity of $H_\alpha$ line measured around filaments by emission spectroscopy and (d) density of the $H^0$ atoms estimated from the $H_\alpha$ line by CR model.

# 4. Experimental Results

## 4.1 Longitudinal distribution

Figures 4 (a) and (b) show typically longitudinal distributions of electron temperature ($T_e$) and ion saturation current ($J_{is}$ ($H^+$ ions)) at $X = 0$ mm and $Z = 15$ mm, respectively. Figure 4 (c) shows the distribution of the intensity of $H_\alpha$ (656 nm) line emission measured around filaments.

The $T_e$ is locally high at $-500 < Y < -400$ mm and constant at $Y > -400$ mm. The $J_{is}$ is also locally high at the same region of $-500 < Y < -400$ mm giving the high $T_e$, and nearly constant of 150 A/m$^2$ at $-400 < Y < 0$ mm and quite low at $Y > 0$. This upward localization of the source plasma is similar to that of the calculated population of the primary electrons in the longitudinal direction as shown in Fig. 3 (b).

As shown in Fig. 4 (c), the distribution of the inten-

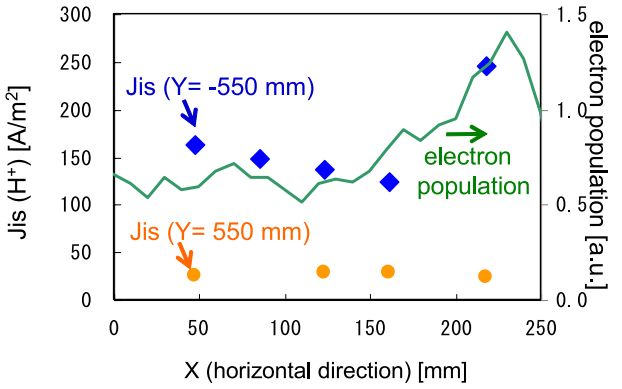


Fig. 5 Horizontal distributions of $J_{is}$ ($H^+$) measured at $Y = -550$ mm (top of the ion source) and $Y = 550$ mm (bottom of the ion source) by the Langmuir probes. Calculated electron population at $Y = -550$ mm is shown as the solid line.

sity of H$\alpha$ line emission around filaments is constant in the longitudinal direction. From the measured intensity of the $H_\alpha$ line, the density of the $H^0$ atoms is estimated by CR model [9, 10]. In this calculation, the $H_\alpha$ line is simply assumed to be only emitted by excitation of the $H^0$ atoms, which mainly occur in the source plasma, although the light is also emitted from dissociation of the $H_2$ molecules by electron collisions and from recombination of $H^+$ ions and electrons. In this case, the density of the $H^0$ atoms is determined by the intensity of H$\alpha$ line emission, electron temperature and density of the electrons. The electron temperature is assumed to be 5 eV that is the typical value in the arc condition [11]. The density of the electron is evaluated from the measured values. The estimated density of the $H^0$ atoms is plotted along the longitudinal direction in Fig. 4 (d). The distribution of the $H^0$ atoms shows the localization in the top of the arc chamber and the similar tendency of the $H^+$ ion distribution. This suggests that the plasma localization results in the localization of the $H^0$ atoms.

### 4.2 Horizontal distribution

Figure 5 shows the horizontal distributions of $H^+$ ions ($J_{is}$) in the top and bottom of the arc chamber. In this figure, the calculated horizontal distribution of primary electron is shown as the solid line. In the $Y = -550$ mm (top of the arc chamber), $H^+$ ions ($J_{is}$) are relatively high. Particularly near the side wall of the top of the arc chamber, the $H^+$ ions are highly localized. The primary electron population is also localized in the same region as the distribution of the $J_{is}$, resulting in the localization of the $H^0$ atoms. The localization of the $H^+$ ions and $H^0$ atoms suggests a relatively high density of the $H^-$ ions near the side wall of the top. In the $Y = 550$ mm (bottom of the arc chamber), the $J_{is}$ is relatively low in the horizontal direction. From the same discussion for the top of the arc chamber, the $H^-$ ions could be relatively low in the bottom of the arc chamber.

## 5. Discussion

From the calculation and the experiment, the origin of beam non-uniformity was discussed. In the arc chamber, it was found that the $H^+$ ions and $H^0$ atoms were localized. According to results in the JAEA 10 A negative ion source with 1/3 scale of the JT-60 negative ion sources with Cs [8], negative ion beam intensity was relatively high in the upper region, where the Te and plasma density were relatively high. This indicates that large amount of the negative ions are produced on the Cs seeded surface in this region without significant destruction by collision with the fast electrons. Accordingly, the plasma localization observed in the present work could lead to the non-uniformity of the negative ions. The non-uniformity of the negative ions causes a poor beam optics of negative ions locally, resulting in direct interception of the beams on the acceleration grids. This is one of the reason why the accelerated negative ion beam is non-uniform.

## 6. Summary

The distribution of $H^+$ ions and $H^0$ atoms, which were parent particles of $H^-$ ions on the cesium covered surface, were measured by Langmuir probes and emission spectroscopy to investigate the origin of the non-uniformity of the source plasmas in the JT-60 negative ion source. As a result, both of $H^+$ ions and $H^0$ atoms were localized at the top of the ion source. The analyses of the primary electron trajectories showed that this non-uniformity was due to the B x grad B drift of primary electrons emitted from filaments. It is suggested that the localization of $H^+$ ions and $H^0$ atoms leads to the non-uniformity of the negative ions in the arc chamber.

To improve the non-uniformity of the negative ions by suppressing the localization of the primary electron due to B x grad B drift, a tent-shaped magnetic filter was effective tested in JAEA 10 A negative ion source with 1/3 scale of the JT-60 negative ion sources [8, 12]. From this result, the tent-shaped filter will be applied to the JT-60 negative ion source.

[1] M. Hanada *et al.*, J. Plamsa Fusion Res. SERISE **9**, 208 (2010).
[2] A. Kojima *et al.*, Rev. Sci. Instrum. **81**, 02B112 (2010).
[3] A. Kojima *et al.*, Rev. Sci. Instrum. **51**, 083049 (2011).
[4] Y. Ikeda *et al.*, Nucl. Fusion **46**, S211 (2006).
[5] M. Kuriyama *et al.*, Fusion Eng. Des. **39-40**, 115 (1998).
[6] Field Precision LLC, http://www.fieldp.com/magnum.html
[7] A. Kojima *et al.*, in: Proceeding of the 27th Symposium on Fusion Technology (2012).
[8] M. Hanada, T. Seki *et al.*, Nucl. Fusion **46**, S318 (2006).
[9] T. Fujimoto *et al.*, J. Appl. Phys. **66**, 2315 (1989).
[10] T. Shibata *et al.*, in: Proceeding of the 3rd International Symposium on Negative Ions, Beams and Sources (2012).
[11] N. Takado *et al.*, J. Appl. Phys. **103**, 053302 (2008).
[12] H. Tobari, M. Hanada *et al.*, Rev. Sci. Instrum. **79**, 02C111 (2008).